

Magnetic field evolution in spatially inhomogeneous axion structures

Petr Akhmetiev^{a,b} and Maxim Dvornikov^{b*}

^a Tikhonov Moscow Institute of Electronics and Mathematics,
National Research University “Higher School of Economics”, Moscow, Russia;

^b Pushkov Institute of Terrestrial Magnetism, Ionosphere
and Radiowave Propagation (IZMIRAN),
108840 Moscow, Troitsk, Russia

Abstract

We study the time evolution of magnetic fields in various configurations of axions with spatially inhomogeneous wavefunctions. The generalization of the induction equation for the magnetic field is derived for such systems. Basing on this equation, we study, first, the evolution of two Chern-Simons (CS) waves interacting with a linearly decreasing axion wavefunction. The nonzero gradient of axions results in the mixing between these CS waves. Then, we consider the problem in a compact domain, when an initial CS wave is mirror symmetric. In this situation, the inhomogeneity of axions acts as the effective modification of the α -dynamo parameter. Thus, we conclude that the influence of spatially inhomogeneous axion on the magnetic field evolution strongly depends on the geometry of the system.

1 Introduction

The most prominent solution of the CP problem in quantum chromodynamics (QCD) requires the existence of a pseudoscalar particle called the axion [1]. Nowadays axions and axion like particles are one of the most reliable candidates for the dark matter particles [2]. Despite numerous attempts to directly detect an axion in an experiment, these particles still remain elusive. The main experimental techniques used for the axion detection are reviewed in Ref. [3]. The role of axions in astrophysics is highlighted in Ref. [4].

As a rule, axions in the early universe are spatially homogeneous. However, the coordinate dependence of the axion field is not ruled out [5]. It can be the case when the Peccei-Quinn (PQ) phase transition happens after the reheating during the inflation. In the present work, we consider such a situation when axions form spatially confined objects. One of the examples of such structures are the axion stars [6], which are the solutions of the wave equation for an axion field in curved spacetime accounting for a self-interaction of axions. Another possibility for these objects are axion miniclusters [7] which are made of virialized axions. The characteristics of the axion miniclusters were recently studied in Refs. [8,9]. The impact of the axions inhomogeneity on the properties of cold dark matter was studied in Ref. [10].

*maxdvo@izmiran.ru

Axions turn out to interact not only with quarks and between themselves but also with photons. The most general couplings between axions and photons are provided, e.g., in Ref. [11]. The interaction of axions and primordial magnetic fields was studied in Refs. [12,13]. The instabilities in the axion MHD are discussed in Ref. [14]. We studied the interaction between inhomogeneous axions and helical primordial magnetic fields in Ref. [15]. We assumed in Ref. [15] that the spatial inhomogeneity of axions was isotropic, i.e. the mean value of the wavefunction gradient vanishes whereas the Laplace operator survives.

In the present work, basing on the results of Ref. [15], we consider the mutual evolution of a magnetic field and axions having the fixed spatial distributions. It can correspond, e.g., to an axion star. For this purpose, we consider two situations: the simplified one dimensional model and the more sophisticated geometry based on the Hopf fibration.

Magnetic fields on 3D sphere relate with the Hopf fibration and are considered in numerous works (see, e.g., Ref. [16, Ch. III] and references therein). In Ref. [17], a simplest hyperbolic analogue of the Hopf fibration is applied to construct the magnetic equilibrium on the 3D sphere with the variations of the magnetic permeability. Such a hyperbolic Hopf fibrations are based on the Ghys-Dehornoy examples of geodesic flows.

In Ref. [19], the Hopf fibration is used to translate solutions in a compact domain to solutions in the standard 3D space. We develop this task in Sec. A. Our approach is different from that in Ref. [19], where the magnetic vector potential \mathbf{A} is transformed. We use the Kelvin transformation to construct the magnetic field \mathbb{B} in the Euclidean space with various magnetic permeabilities and regular boundary conditions at the infinity. This approach keeps the magnetic helicity and admits magnetic energy calculations analogously to Ref. [17]. Because of various magnetic permeabilities, the operator curl in the Euclidean space is a non-standard and calculations are different with respect to Sec. 3.

In our present construction, the configuration is elliptic, i.e. a scalar curvature parameter in a compact domain is positive, and higher invariants of magnetic lines are unnecessary. Using the idea from Ref. [18], the higher invariants of magnetic lines are required for fields with the $SU(2)$ symmetry.

Because the initial Chern-Simons (CS) configuration in this domain is mirror symmetric, i.e. the linking numbers for an arbitrary pair of magnetic lines equal to zero, the helicity flow is completely characterized by a flow of the dispersion of the asymptotic ergodic Hopf invariant.

In Ref. [20], the analytic formula for the dispersion of the ergodic asymptotic Hopf invariant, or, the magnetic helicity density is proposed. We recall that the Hopf invariant [16] is a density of linking numbers of pairs of magnetic lines. The magnetic helicity density has the dimension $G^2\text{cm}^{-2}$ and is distributed over 4-dimensional configurations. Initial points of magnetic lines in a pair are translated by a prescribed magnetic flow independently. Thus, the Hopf invariant is distributed at transverse sections of pairs of magnetic lines. However, the dispersion of the Hopf invariant is insufficiently studied since its analytic expression involves an infinite-dimensional space of jets. It is not represented by a finite-dimensional integral [21]. A conception of the asymptotic ergodic Hopf invariants assumes that magnetic lines could be non-closed and integrals over magnetic flow are considered for quasi-periodic functions. For an infinite-dimensional space of jets additional mathematics are required, in [22] an approach for non-periodic observables is developed.

The dispersion of the magnetic helicity density, as it is shown in Ref. [20], has the dimension $G^4\text{cm}^{-4}$. It is distributed over the 5-dimensional configuration space, where initial points of magnetic lines in a pair are simultaneously translated by the magnetic flow. The

spatial factor 4/5 shows the quadratic magnetic helicity spectra is more energetic. A flow of the magnetic helicity density given by the axion interactions will be considered elsewhere.

The present work is organized in the following way. In Sec. 2, we briefly remind how magnetic fields evolve under the influence of inhomogeneous axions. We consider the simple one dimensional model in Sec. 3. Then, in Secs. 4 and 5, we qualitatively study a more complicated 3D case. Finally, we conclude in Sec. 6. The Kelvin transformation is considered in Appendix A.

2 Electrodynamics in presence of inhomogeneous axions

The equations of the axion electrodynamics in a curved spacetime have the form,

$$\begin{aligned} \frac{1}{\sqrt{-g}}\partial_\nu(\sqrt{-g}F^{\mu\nu}) + g_{a\gamma}\partial_\nu\varphi\tilde{F}^{\mu\nu} + J^\mu &= 0, \\ \frac{1}{\sqrt{-g}}\partial_\nu(\sqrt{-g}\tilde{F}^{\mu\nu}) &= 0, \\ \frac{1}{\sqrt{-g}}\partial_\mu(\sqrt{-g}\partial^\mu\varphi) + m^2\varphi + \frac{g_{a\gamma}}{4}F_{\mu\nu}\tilde{F}^{\mu\nu} &= 0, \end{aligned} \quad (2.1)$$

where $F_{\mu\nu}$ is the electromagnetic field tensor, $\tilde{F}^{\mu\nu} = \frac{1}{2}E^{\mu\nu\alpha\beta}F_{\alpha\beta}$, $E^{\mu\nu\alpha\beta} = \frac{1}{\sqrt{-g}}\varepsilon^{\mu\nu\alpha\beta}$ is the covariant antisymmetric tensor, $\varepsilon^{0123} = +1$, $g = \det(g_{\mu\nu})$, $g_{\mu\nu} = \text{diag}(1, -a^2, -a^2, -a^2)$ corresponds to the Friedmann-Robertson-Walker (FRW) metric with the scale factor $a(t)$, $g_{a\gamma}$ is the coupling constant, $J^\mu = (\rho, \mathbf{J}/a)$ is the external current, φ is the axion wavefunction, and m is the axion mass.

Using the conformal variables [23], $\mathbf{E}_c = a^2\mathbf{E}$, $\mathbf{B}_c = a^2\mathbf{B}$, $\rho_c = a^3\rho$, and $\mathbf{J}_c = a^3\mathbf{J}$, and applying the results of Ref. [15], we derive the equation for \mathbf{B}_c ,

$$\mathbf{B}'_c = \nabla \times [\mathbf{b} \times (\nabla \times \mathbf{B}_c) + \alpha\mathbf{B}_c - \eta_m(\nabla \times \mathbf{B}_c)]. \quad (2.2)$$

where $\mathbf{b} = g_{a\gamma}\nabla\varphi/\sigma_c^2$, $\alpha = g_{a\gamma}\varphi'/\sigma_c$ is the analogue of the α -dynamo parameter, $\eta_m = \sigma_c^{-1}$ is the magnetic diffusion coefficient, $\sigma_c \approx 10^2 T_{\text{CMB}}$ is the conformal conductivity of ultrarelativistic plasma, $T_{\text{CMB}} = 2.7\text{K}$ is the current temperature of the cosmic microwave background radiation, and the prime means the derivative with respect to the conformal time η defined by $dt = a d\eta$. For example, we can choose $a = T_{\text{CMB}}/T$ and $\eta = \tilde{M}_{\text{Pl}} T_{\text{CMB}}^{-1} (T^{-1} - T_{\text{QCD}}^{-1})$, where $\tilde{M}_{\text{Pl}} = M_{\text{Pl}}/1.66\sqrt{g_*}$, $M_{\text{Pl}} = 1.2 \times 10^{19}\text{GeV}$ is the Planck mass, and $g_* = 17.25$ is the number of the relativistic degrees of freedom at the QCD phase transition [24], which happens at $T_{\text{QCD}} \approx 100\text{MeV}$. In this case $\eta(T_{\text{QCD}}) = 0$ and $a_{\text{now}} \equiv a(T_{\text{CMB}}) = 1$.

In Eq. (2.2), we keep only the terms linear in φ . Note that \mathbf{B}_c in Eq. (2.2) always has the zero divergence, $(\nabla \cdot \mathbf{B}_c) = 0$. We add to Eq. (2.2) the equation for the evolution of φ which has the form,

$$\varphi'' + 2H\varphi' - \nabla^2\varphi + a^2m^2\varphi = \frac{g_{a\gamma}}{a^2}(\mathbf{E}_c\mathbf{B}_c), \quad (2.3)$$

where $H = a'/a$ is the Hubble parameter. We study axions after the QCD phase transition when their mass are independent of the plasma temperature.

In Ref. [15], we considered the electrodynamics of inhomogeneous axions by assuming that distribution of their wavefunction is isotropic, i.e. we supposed that only even number of derivatives, like $\partial_i\partial_j\varphi$ etc., is nonzero. Now, our task is to study the impact of the term $\mathbf{b} \propto \nabla\varphi$ in Eq. (2.2) on the evolution of the magnetic field. For this purpose, we study a spatially confined axion structure like an axion star.

3 One dimensional model

We consider the situation when the magnetic field is the superposition of two CS waves along the z -axis, which coincides with the radial direction,

$$\mathbf{B}_c = \mathbf{B}_+ + \mathbf{B}_-, \quad \mathbf{B}_+ = B_+^{(0)}(\sin kz, \cos kz, 0), \quad \mathbf{B}_- = B_-^{(0)}(\cos kz, -\sin kz, 0), \quad (3.1)$$

where the amplitudes are functions of conformal time $B_{\pm}^{(0)} = B_{\pm}^{(0)}(\eta)$ and k is the wave vector characterizing the scale of the system $\propto k^{-1}$. Note that $(\mathbf{B}_+ \cdot \mathbf{B}_-) = 0$, i.e. these waves correspond to different polarizations. We assume that $\nabla\varphi$ is also along the z -axis, i.e. $\mathbf{b} = (0, 0, b)$. Thus, we get the following system of differential equations:

$$B_+^{(0)'} = k \left[kbB_-^{(0)} + B_+^{(0)}(\alpha - \eta_m k) \right], \quad B_-^{(0)'} = k \left[-kbB_+^{(0)} + B_-^{(0)}(\alpha - \eta_m k) \right], \quad (3.2)$$

for the amplitudes of CS waves. We can see in Eq. (3.2) that the nonzero gradient of the axion $b \propto \partial_z \varphi$ mixes the independent CS waves.

The distribution of the axion inside of an axion star can be quite sophisticated (see, e.g., Ref. [25]). We adopt the simple model, in which the axion wavefunction has the form,

$$\varphi(z, \eta) = \begin{cases} \varphi_0(\eta), & 0 < z < R, \\ \varphi_0(\eta) \left(1 - \frac{z-R}{\Delta}\right), & R < z < R + \Delta, \\ 0, & z > R + \Delta, \end{cases} \quad (3.3)$$

where R is the radius of the axion star core, Δ is the depth of the stellar crust, which is supposed to be thin, $\Delta \ll R$, and $\varphi_0(\eta)$ is the oscillating amplitude of the wavefunction. It means that we consider the analogue of the α -dynamo in a thin layer (see, e.g., Ref. [26]). Using the fact that $\mathbf{E}_c = \mathbf{J}_c/\sigma_c = (\nabla \times \mathbf{B}_c)/\sigma_c$ and Eq. (3.1), we get that $(\mathbf{E}_c \cdot \mathbf{B}_c) = k(B_+^{(0)2} + B_-^{(0)2})/\sigma_c$ in Eq. (2.3).

Basing on Eq. (3.3), we obtain that $b = -g_{a\gamma}\varphi_0/\Delta\sigma^2$ and $\nabla^2\varphi \equiv \partial_z^2\varphi = 0$. Finally, Eqs. (2.3) and (3.2) are rewritten in the form,

$$\begin{aligned} B_+^{(0)'} &= \frac{k}{\sigma_c} \left[-\frac{g_{a\gamma}k\varphi_0}{\Delta\sigma_c} B_-^{(0)} + B_+^{(0)} (g_{a\gamma}\varphi_0' - k) \right], \\ B_-^{(0)'} &= \frac{k}{\sigma_c} \left[\frac{g_{a\gamma}k\varphi_0}{\Delta\sigma_c} B_+^{(0)} + B_-^{(0)} (g_{a\gamma}\varphi_0' - k) \right], \\ \varphi_0'' &= -2H\varphi_0' - a^2m^2\varphi_0 + \frac{g_{a\gamma}k}{a^2\sigma_c} (B_+^{(0)2} + B_-^{(0)2}). \end{aligned} \quad (3.4)$$

To derive Eq. (3.4) we take that we are at the bottom of the stellar crust, i.e. $z \gtrsim R$.

Using the dimensionless variables

$$B_{\pm}^{(0)} = \frac{k}{g_{a\gamma}} \mathcal{B}_{\pm}, \quad \varphi_0 = \frac{\sigma_c}{kg_{a\gamma}} \Phi, \quad \eta = \frac{\sigma_c}{k^2} \tau, \quad (3.5)$$

we rewrite Eq. (3.4) in the form,

$$\frac{d\mathcal{B}_+}{d\tau} = -K\Phi\mathcal{B}_- + \mathcal{B}_+ (\xi\Psi - 1), \quad (3.6)$$

$$\frac{d\mathcal{B}_-}{d\tau} = K\Phi\mathcal{B}_+ + \mathcal{B}_- (\xi\Psi - 1), \quad (3.7)$$

$$\frac{d\Psi}{d\tau} = -\beta\Psi - \mu^2a^2\Phi + \frac{1}{a^2} (\mathcal{B}_+^2 + \mathcal{B}_-^2), \quad (3.8)$$

where $\Psi = \partial_\tau \Phi$, $\mu = m\sigma_c/k^2$ is the dimensionless axion mass, $K = (\Delta k)^{-1}$, and $\beta = 2H\sigma_c/k^2$. The terms $\mathcal{B}_\pm\Psi$ in the right hand side of Eqs. (3.6) and (3.7) are responsible for the dynamo amplification of the magnetic field, i.e. the magnetic field becomes unstable. That is why, following Ref. [27], we introduce the quenching factor $\xi = [1 + (\mathcal{B}_+^2 + \mathcal{B}_-^2)/\mathcal{B}_{\text{eq}}^2]^{-1}$ in these terms. Here \mathcal{B}_{eq} is the equipartition magnetic field.

The numerical solution of Eqs. (3.6)-(3.8) requires the initial conditions. First, we establish the initial condition for axions. The energy-momentum tensor of axions is

$$T_{\mu\nu} = \partial_\mu\varphi\partial_\nu\varphi - \frac{g_{\mu\nu}}{2}(g^{\lambda\rho}\partial_\lambda\varphi\partial_\rho\varphi - m^2\varphi^2). \quad (3.9)$$

Using Eq. (3.9), we get that the total axions energy density is

$$\rho_a = T_{00} = \frac{1}{2} \left[\dot{\varphi}^2 + \frac{1}{a^2}(\nabla\varphi)^2 + m^2\varphi^2 \right]. \quad (3.10)$$

We suppose that $\dot{\varphi} = 0$ initially. Thus, the initial energy density is

$$\rho_a^{(0)} \approx \frac{\varphi_0^2}{2a^2\Delta^2}(1 + m^2a^2\Delta^2). \quad (3.11)$$

We can compare this quantity with $(\varepsilon m f_a)^2$, where the factor $\varepsilon \sim 10^{-10}$ for a dilute star and $\varepsilon \sim 1$ for a dense one (see, e.g., Ref. [28]). Thus, we get the initial condition for the axion field in terms of the dimensionless variables

$$\Phi(T = T_{\text{QCD}}) = \frac{\alpha_{\text{em}}\varepsilon m a \Delta k}{\pi\sigma_c\sqrt{2(1 + m^2a^2\Delta^2)}}, \quad \Psi(T = T_{\text{QCD}}) = 0. \quad (3.12)$$

Here, we use the relation, $g_{a\gamma} \approx \frac{\alpha_{\text{em}}}{2\pi f_a}$, where $\alpha_{\text{em}} = 7.3 \times 10^{-3}$ is the fine structure constant and f_a is the PQ constant.

We suppose that the stellar crust has the width $\Delta = 0.1R$. The parameter k in Eq. (3.1) is related to radius of the core as $k = R^{-1}$. It means that $K = 10$ in Eqs. (3.6)-(3.8). We take that $k = 10^{-8}T_{\text{CMB}}$, which is much less than the reciprocal Debye scale $k_{\text{D}} = 10^{-1}T_{\text{CMB}}$. The physical size of such a star, if it would evolve to the present time, is ~ 85 km.

The axion mass is taken to be $m = 10^{-3}$ eV, which is below the upper bound established in Ref [29]. Moreover, we use the approximate relation (see, e.g., Ref. [30])

$$\left(\frac{m}{10^{-6} \text{ eV}} \right) \approx 5.7 \left(\frac{f_a}{10^{12} \text{ GeV}} \right)^{-1}, \quad (3.13)$$

between the axion mass and the PQ constant.

We suppose that the conformal seed magnetic field is $B_+^{(0)}(T = T_{\text{QCD}}) = 4.4 \times 10^{13}$ G and $B_-^{(0)}(T = T_{\text{QCD}}) = 0$, i.e. only one CS wave in Eq. (3.1) is present initially. We use the seed strength equal to the Schwinger value $B_{\text{crit}} = m_e^2/e$. The value of the equipartition field is taken in the range $\mathcal{B}_{\text{eq}} \lesssim 10^{-5}$.

We remind that our main goal is to study the behavior of the magnetic field under the influence of axions with a nonzero $\nabla\varphi$. That is why, first, we plot the amplitudes of CS waves $B_\pm^{(0)}$ versus the temperature of primordial plasma T for a dense axion star in Fig. 1(a) and for a dilute one in Fig. 1(b). We can see that these cases coincide qualitatively. The insets in Fig. 1 show the behavior of the magnetic field at short evolution times. They confirm our guess that a nonzero $\nabla\varphi$ mixes two different CS waves.

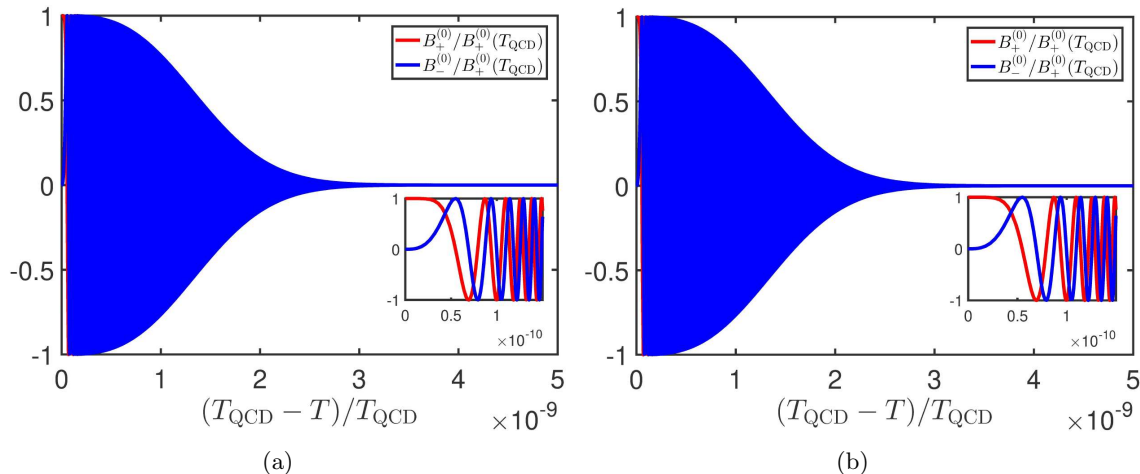


Figure 1: The evolution of $B_{\pm}^{(0)}$ in primordial plasma after the QCD phase transition. Red and blue lines correspond to $B_{+}^{(0)}$ and $B_{-}^{(0)}$ normalized by $B_{+}^{(0)}(T_{\text{QCD}})$. The insets show the behavior of $B_{\pm}^{(0)}$ at short evolution time. The parameters of the system are $m = 10^{-3}$ eV, $\Delta = 0.1R$, $k = 10^{-8}T_{\text{CMB}}$, $B_{+}^{(0)}(T_{\text{QCD}}) = 4.4 \times 10^{13}$ G and $B_{-}^{(0)}(T_{\text{QCD}}) = 0$. Panel (a) corresponds to a dense star; panel (b) to a dilute one.

The magnetic fields in Fig. 1 decay quite rapidly. It happens because of both the magnetic diffusion and the magnetic field quenching in Eqs. (3.6) and (3.7). To demonstrate this fact avoiding the rapid oscillations visible in Fig. 1, we show the evolution of the total magnetic energy $\Xi_{\text{B}} \propto B_{+}^{(0)2} + B_{-}^{(0)2}$ in Fig. 2. Again, both dense and dilute axion stars are considered.

Finally, in Fig. 3, we depict the axion energy, defined in Eq. (3.10), for a dense and dilute axion stars. First, we can see in Fig. 3 that axions start oscillating with a frequency much lower than the magnetic field in Fig. 1. We also mention two facts: (i) axions continue oscillating even when the magnetic field decays; and (ii) the function Ξ_a is normalized to its maximal value, which turns out to be great, $\Xi_a^{(\text{max})} \gg 1$. Such behavior of the axion energy results from the term $\propto (\mathcal{B}_{+}^2 + \mathcal{B}_{-}^2) / a^2$ in the right hand side of Eq. (3.8). Before the decay of the magnetic field, shown in Fig. 2, it succeeds to transmit its energy to axions.

Unfortunately, it is technically difficult to trace the evolution of the system at greater times numerically since we have two different typical frequencies: one of them is related to magnetic field oscillations, cf. Fig. 1, another one to axion oscillations. The ratio of these frequencies is huge.

4 Three dimensional model based on a spherical CS wave

In this section, we qualitatively consider the evolution of 3D magnetic fields under the influence of inhomogeneous axions. We have demonstrated in Sec. 3 that the seed magnetic field decays quite rapidly; cf. Figs. 1 and 2. That is why we neglect the conformal quantities and consider the physical magnetic fields.

By a spherical CS wave we means an analogue of CS waves in Eq. (3.1), which is defined in a compact domain rather than in the flat Euclidean space. The simplest example of a closed

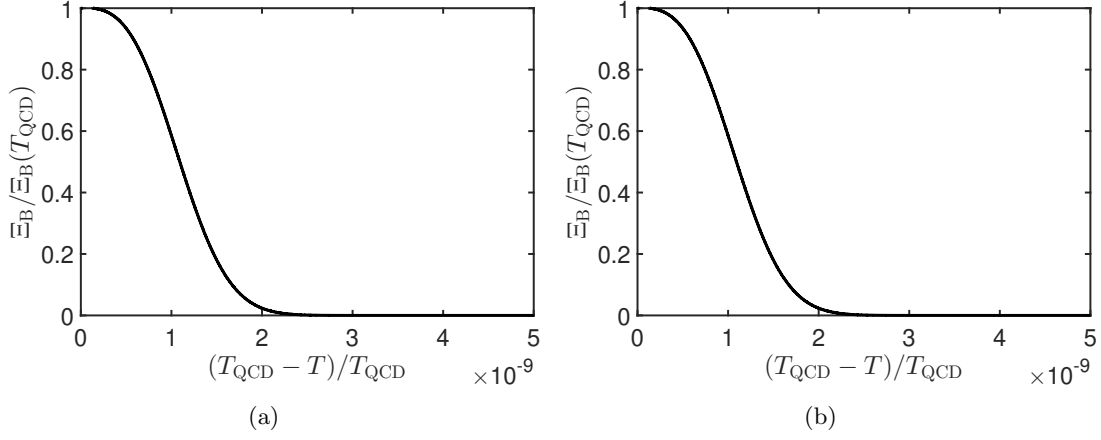


Figure 2: The evolution of the total magnetic energy density $\Xi_B \propto B_+^{(0)2} + B_-^{(0)2}$ normalized by its initial value. The parameters of the system are the same as in Fig. 2. Panel (a) corresponds to a dense star; panel (b) to a dilute one.

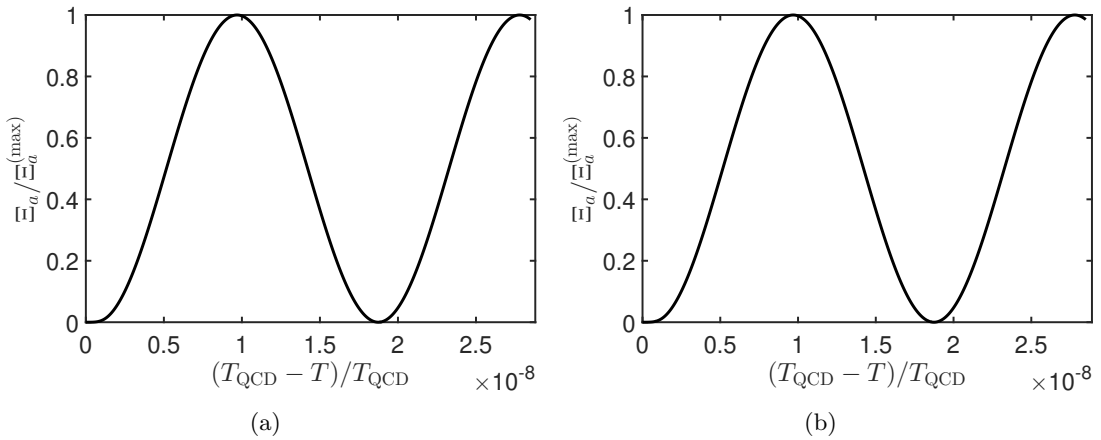


Figure 3: The axion energy density Ξ_a , normalized by its maximal value, versus the plasma temperature. The parameters of the system are the same as in Fig. 2. Panel (a) corresponds to a dense star; panel (b) to a dilute one.

compactified 3D domain is the standard 3D unite sphere, which is defined in 4D Euclidean space with the coordinates (x_0, x_1, x_2, x_3) by the equation:

$$x_0^2 + x_1^2 + x_2^2 + x_3^2 = 1. \quad (4.1)$$

On the unite 3D sphere, we define right, \mathbf{B}_+ , and left, \mathbf{B}_- , magnetic fields, as well as the following non-helical magnetic fields: $\mathbf{B}_A = \mathbf{B}_+ - \mathbf{B}_-$ and $\mathbf{B}_B = \mathbf{B}_+ + \mathbf{B}_-$. The magnetic field \mathbf{B}_A is not a complete analogue of the vector \mathbf{B}_c , given by Eq. (3.1), because the vector \mathbf{B}_c is a right-polarized in the case $k > 0$, whereas the vector \mathbf{B}_A is a mirror-symmetric. An interesting fact that \mathbf{B}_A is orthogonal to \mathbf{B}_B and the two magnetic modes are linked by the helicity integral. Let us remark that the magnetic vector \mathbf{B}_+ is well-known and was constructed in Ref. [16, Ex. 1.9, Ch. III], as well as in Ref. [19], using the Kelvin transformation described in Appendix A. The splitting

$$\mathbf{B}_+ = \frac{1}{2}[\mathbf{B}_A + \mathbf{B}_B], \quad (4.2)$$

into the sum of two mirror-symmetric vectors is new.

Unfortunately, in a compact domain, we are not able the define a regular analogue of the gradient of the axion wavefunction \mathbf{b} as in Eq. (2.2). The simplest analogue of the vector shift is the k -spectrum of the magnetic field. Instead of the evolution Eq. (3.2) we get a nonlinear oscillator, determined by an infinite numbers of harmonics.

We describe the analogue of Eq. (3.4). Then, we calculate the first-order derivative of a solution in the right-hand side of the equation using the vector \mathbf{b} in the left hand side of the equation. The axion density energy in the case is given analogously with Eq. (2.3). This solution can be used to describe the evolution of the magnetic field in a short time, when an initial magnetic is slowly varying, whereas the axion density energy changes rapidly. Analogous situation was studied in Ref. [15]. Thus, here, we consider the situation opposite to that shown in Figs. 1 and 3.

To define a spherical analogue of a CS wave we use standard MHD calculations on the Riemannian manifold given in Ref. [16, Def. 5.9, Ch. 1]. The standard 3D sphere of the unit radius is equipped by the following coordinate system $(\phi, \psi, \theta = 2\chi)$, which is related with the Cartesian coordinate system in \mathbb{R}^4 by Eq. (4.7).

Let us define the curves Θ_A and Θ_B on \mathbb{R}^4 rather than on \mathbb{C}^2 ,

$$\begin{aligned} \Theta_A(\phi; x_0, x_1, x_2, x_3) &= \Theta_A(\phi; x_0, x_1) = (R_A \cos(\phi), R_A \sin(\phi), 0, 0), \\ \Theta_B(\psi; x_0, x_1, x_2, x_3) &= \Theta_B(\psi; x_2, x_3) = (0, 0, R_B \cos(\psi), R_B \sin(\psi)). \end{aligned} \quad (4.3)$$

Since $R_A^2 + R_B^2 = 1$, let us put $R_A = \sin(2\chi)$ and $R_B = \cos(2\chi)$. Thus, we can compute

$$\mathbf{B}_A = d\Theta_A/d\phi, \quad \mathbf{B}_B = d\Theta_B/d\psi. \quad (4.4)$$

Using Eq. (4.4), we define the associated differential one-forms on \mathbb{R}^4 ,

$$\beta_A^{\mathbb{R}^4} = B_A^0 dx^0 + B_A^1 dx^1 = -\sin(\phi)R_A dx^0 + \cos(\phi)R_A dx^1. \quad (4.5)$$

$$\beta_B^{\mathbb{R}^4} = B_B^2 dx^2 + B_B^3 dx^3 = -\sin(\psi)R_B dx^2 + \cos(\psi)R_B dx^3. \quad (4.6)$$

We now define the mapping between points on the three-sphere S^3 and \mathbb{R}^4 ,

$$\begin{aligned}
\Upsilon &= (x_0, x_1, x_2, x_3), \\
x_0 &= \cos(\phi) \cos(2\chi), \\
x_1 &= \sin(\phi) \cos(2\chi), \\
x_2 &= \cos(\psi) \sin(2\chi), \\
x_3 &= \sin(\psi) \sin(2\chi),
\end{aligned} \tag{4.7}$$

with the coordinates of S^3 : $\phi \in [0, 2\pi)$, $\psi \in [0, 2\pi]$, and $2\chi \in [0, \frac{\pi}{2}]$. We can now compute the differential one-forms $\beta_A^{\mathbb{R}^4}$ and $\beta_B^{\mathbb{R}^4}$ on S^3 as the pull-back under the mapping Υ ,

$$\begin{aligned}
\beta_A^{S^3} &= \Upsilon^* \beta_A^{\mathbb{R}^4} \\
&= \sin(\phi) \cos(2\chi) \sin(\phi) \cos(2\chi) \mathbf{d}\phi + \sin(\phi) \cos(2\chi) \cos(\phi) \sin(2\chi) \mathbf{d}2\chi \\
&\quad + \cos(2\chi) \cos(\phi) \cos(\phi) \cos(2\chi) \mathbf{d}\phi - \cos(2\chi) \cos(\phi) \sin(\phi) \sin(2\chi) \mathbf{d}2\chi \\
&= \cos^2(2\chi) \mathbf{d}\phi,
\end{aligned} \tag{4.8}$$

$$\begin{aligned}
\beta_B^{S^3} &= \Upsilon^* \beta_B^{\mathbb{R}^4} \\
&= \sin(\psi) \sin(2\chi) \sin(\psi) \sin(2\chi) \mathbf{d}\phi - \sin(\psi) \sin(2\chi) \cos(\psi) \cos(2\chi) \mathbf{d}2\chi \\
&\quad + \cos(\psi) \sin(2\chi) \cos(\psi) \sin(2\chi) \mathbf{d}\phi + \cos(\psi) \sin(2\chi) \sin(\psi) \cos(2\chi) \mathbf{d}2\chi \\
&= \sin^2(2\chi) \mathbf{d}\psi.
\end{aligned} \tag{4.9}$$

The forms in Eqs. (4.8) and (4.9) obey the properties,

$$\mathbf{d}\beta_A^{S^3} = -2 \cos(2\chi) \sin(2\chi) \mathbf{d}2\chi \wedge \mathbf{d}\phi, \tag{4.10}$$

$$\mathbf{d}\beta_B^{S^3} = 2 \cos(2\chi) \sin(2\chi) \mathbf{d}2\chi \wedge \mathbf{d}\psi. \tag{4.11}$$

We take their Hodge-dual $\star \mathbf{d}\beta_A^{S^3}$, with the volume element $\mathbf{d}V = \cos 2\chi \sin(2\chi) \mathbf{d}\phi \wedge \mathbf{d}2\chi \wedge \mathbf{d}\psi$, and find

$$\star \mathbf{d}\beta_A^{S^3} = \frac{1}{2} \sin^2(2\chi) \cos^2(2\chi) \mathbf{d}\psi = 2 \sin^2(4\chi) \mathbf{d}\psi, \tag{4.12}$$

$$\star \mathbf{d}\beta_B^{S^3} = -\frac{1}{2} \sin^2(2\chi) \cos^2(2\chi) \mathbf{d}\phi = 2 \sin^2(4\chi) \mathbf{d}\phi. \tag{4.13}$$

Finally, we get the result,

$$\mathbf{d} \star \mathbf{d}\beta_A^{S^3} = 2 \mathbf{d}\beta_B^{S^3}, \tag{4.14}$$

$$\mathbf{d} \star \mathbf{d}\beta_B^{S^3} = 2 \mathbf{d}\beta_A^{S^3}. \tag{4.15}$$

Let us define smooth magnetic fields

$$\begin{aligned}
\mathbf{B}_+ &= \mathbf{B}_A + \mathbf{B}_B = \star \mathbf{d}\beta_A^{S^3} + \star \mathbf{d}\beta_B^{S^3}, \\
\mathbf{B}_- &= \mathbf{B}_A - \mathbf{B}_B = \star \mathbf{d}\beta_A^{S^3} - \star \mathbf{d}\beta_B^{S^3},
\end{aligned} \tag{4.16}$$

on S^3 , where \star means a vector field, which is associated with the corresponding 2-form by means of the volume form. The quantities \mathbf{B}_A and \mathbf{B}_B are defined using the corresponding 2-form in Eqs. (4.10) and (4.11). Let us define a rescaling, $\mathbf{B}_A \mapsto \frac{1}{2} \mathbf{B}_A$ and $\mathbf{B}_B \mapsto \frac{1}{2} \mathbf{B}_B$, for simplicity.

Using the coordinates $(\phi, \psi, 2\chi = \theta)$ on S^3 , we get that

$$\mathbf{B}_A = (\sin(\theta), 0, 0); \quad \mathbf{B}_B = (0, \cos(\theta), 0). \tag{4.17}$$

Obviously, $\text{curl}(\mathbf{B}_+) = 2\mathbf{B}_+$ and $\text{curl}(\mathbf{B}_-) = -2\mathbf{B}_-$.

5 Harmonics

Let us rescale the latitude θ into χ by the formula,

$$\theta = 2\chi, \quad \theta \in \left[0, \frac{\pi}{2}\right]. \quad (5.1)$$

Let us define the magnetic harmonics $\mathbf{B}_{1,A}$, which are called poloidal harmonics. A poloidal harmonic equals to zero at $\theta = 0$.

It is convenient to remark for the calculations that the absolute value of the vectors $\mathbf{B}_A \cos(\theta)$ and $\mathbf{B}_B \sin(\theta)$ coincides with functions of θ -coordinate and is defined as $\cos(\theta) \sin(\theta)$. Directions of the vectors are perpendicular at an arbitrary point on S^3 .

Let us define the axion wavefunction $\varphi(\theta, t)$, which is a pseudoscalar analogue of Eq. (2.3), on the sphere. It also depends on time by the formula,

$$\varphi(\theta, t) = a_0 \cos(n\theta) \sin(\omega t), \quad (5.2)$$

where the parameter a_0 is assumed to be small.

Since $(\mathbf{B}_A \cdot \mathbf{B}_B) = 0$, the function $\varphi(\theta, t)$ obeys the equation,

$$\ddot{\varphi} - \nabla^2 \varphi + m^2 \varphi = 0, \quad (5.3)$$

and the following expression is valid: $-\omega^2 + n^2 + m^2 = 0$. Note that Eq. (5.3) is analogous to Eq. (2.3) where we neglect the universe expansion.

Let us consider the following sequence of transformations:

$$\begin{aligned} \mathbf{B}_B &\xrightarrow{\text{curl}} 2\mathbf{B}_A \xrightarrow{\times \nabla \cos(n\theta)} -2n \sin(n\theta) \sin(\theta) \cos^{-1}(\theta) \mathbf{B}_B \\ &\xrightarrow{\text{curl}} 2n \frac{d}{d\theta} [\tan(\theta) \sin(n\theta)] \cot(\theta) \mathbf{B}_A - 4n \tan(\theta) \sin(n\theta) \mathbf{B}_A. \end{aligned} \quad (5.4)$$

Basing on Eq. (5.4), we consider the case $n = 2$. In this situation, one has

$$\begin{aligned} \mathbf{B}_B &\xrightarrow{\text{curl}} 2\mathbf{B}_A \xrightarrow{\times \nabla \cos(2\theta)} \\ -8 \sin^2(\theta) \mathbf{B}_B &\xrightarrow{\text{curl}} 16 \cos^2(\theta) \mathbf{B}_A - 16 \sin^2(\theta) \mathbf{B}_A = 16 \cos(2\theta) \mathbf{B}_A. \end{aligned} \quad (5.5)$$

Let us apply the calculations in Eq. (5.5) to the formula:

$$\begin{aligned} \dot{\mathbf{B}}_B &= a_0 \sin(\omega t) \nabla \times [\nabla \cos(n\theta) \times (\nabla \times \mathbf{B}_B)] + \\ &\quad \nabla \times [\alpha \mathbf{B}_B] - \eta_m \sin(\omega t) \nabla \times [\nabla \times \mathbf{B}_B]. \end{aligned} \quad (5.6)$$

where α is defined in Eq. (2.2).

Since $\alpha = \omega \alpha_0 \cos(\omega t) \cos(n\theta)$, for a small α_0 only first-order terms are calculated. The first term is known from Eq. (5.5). The second term is given by $\nabla \times [\alpha \mathbf{B}_B] = \alpha_0 \omega \cos(\omega t) \nabla \times [\cos(n\theta) \mathbf{B}_B] = \omega \alpha_0 \cos(\omega t) [n \sin(n\theta) \sin^{-1}(\theta) \cos(\theta) \mathbf{B}_A + 2 \cos(n\theta) \mathbf{B}_A]$. For $n = 2$ the second term is the following: $-2\omega \alpha_0 \cos(\omega t) [2 \cos^2(\theta) - \sin^2(\theta)] \mathbf{B}_A$. The third term has the form, $-4\eta_m \sin(\omega t) \mathbf{B}_B$.

To simplify the calculations we take $\eta_m = 0$. In the case $n = 2$, we have

$$\dot{\mathbf{B}}_B = 2a_0 [8 \sin(\omega t) \cos(2\theta) + \omega \cos(\omega t) (2 \cos^2(\theta) - \sin^2(\theta))] \mathbf{B}_A. \quad (5.7)$$

Let us transform Eq. (5.7) as

$$2a_0 [8 \sin(\omega t) - \omega \cos(\omega t)] \cos(2\theta) \mathbf{B}_A + 2a_0 \omega \cos(\omega t) \cos^2(\theta) \mathbf{B}_A. \quad (5.8)$$

This calculation means that, in a stationary nonhelical magnetic field \mathbf{B}_B with a fast oscillations of the scalar axion field, a first-order variation is given by a standing wave represented by the second term in Eq. (5.8). The amplitude of the wave is determined by an amplitude of the scalar axion field. Additionally, we get a running wave in the first term in Eq. (5.8). When a frequency ω of the axion field in Eq. (5.7) is great, the α -effect, which is related with the second term in Eq. (5.7) is dominated. Oppositely, when a frequency ω is small, the first term in this equation is dominated. In each of the two limited cases, a standing wave is presented. A running wave is presented when the first and the second term in Eq. (5.7) are of a same order.

6 Conclusion

In the present work, we have studied the simultaneous evolution of magnetic fields and spatially inhomogeneous axionic field. The coordinate dependence of the these fields have been chosen in a specific way imitating realistic situations taking place in astrophysical objects, e.g., in axion stars. We did not study the formation of the fields configuration. Our main goal was to analyze the time evolution of both the magnetic field and the axion wavefunction.

We have started in Sec. 2 with writing down of the main equations of the axion electrodynamics. We have obtained the main Eq. (2.2) for the magnetic field evolution in the presence of a spatially inhomogeneous axion wavefunction. Equation (2.2) is a generalization of the induction equation known in MHD. Our subsequent studies have been based on this equation.

Two main cases have been considered. First, in Sec. 3, we have studied the simplified 1D model where the two CS waves with independent polarizations have been present. The axion wavefunction was linearly decreasing within the crust of an axion star. The main impact of the nonzero gradient of the axion wavefunction in this geometry is the mixing of independent CS waves. It does not contribute to the magnetic field instability.

We have derived the system of ordinary differential equations for the amplitudes of these fields. These system has been solved numerically. We have obtained that the magnetic field decays quite rapidly transferring its energy to axions. This system was supposed to exist in the early universe after the QCD phase transition. However, basing on the results obtained, it is unlikely for any signatures of such an object to evolve to the present days. Moreover, we have obtained that the evolution of dense and dilute axion stars is practically identical.

Then, in Secs. 4 and 5, we have qualitatively studied more complicated situation based on the on the Hopf fibration. In this approach, Eq. (2.3) in a first-order approximation of the solution is satisfied. However, the analogue of the evolution equation (3.4) is different and higher terms of a solution depend on lower ones. Our main result is that, in the chosen geometry, the inhomogeneity of axions leads to the change of the α -dynamo parameter.

In summary, we have found that the impact of the nonzero gradient of the axion wavefunction on the magnetic field evolution strongly depends on the geometry of the system. Of course, the comprehensive analysis should involve the simultaneous solution of both Eqs. (2.2) and (2.3). We plan to tackle this problem in one of our forthcoming works.

Acknowledgments

We are thankful to E. Maslov for useful discussions. The work of P. Akhmetiev is supported by the Russian Science Foundation (Grant No. 21-11-00010).

A The Kelvin transformation

The Kelvin transformation is assumed to be a stereographic projection of the sphere S^3 , outside a marked point pt , into the Euclidean space \mathbb{R}^3 . This transformation is conformal, i.e. an angle between two vectors is unchanged. In Ref. [19], the Kelvin transformation was used to construct the MHD soliton in the Euclidean space with regular conditions at the infinity.

It is remarkable that the Kelvin transformation $T : S^3 \setminus \{pt\} \rightarrow \mathbb{R}^3$ does not modify equations. In the case the marked point pt is the north pole on the sphere: $\psi = \theta = 0$, the magnetic mode \mathbf{B}_A is translated into a (generalized) toroidal mode \mathbb{B}_A , and the magnetic mode \mathbf{B}_B is translated into a (generalized) poloidal mode \mathbb{B}_B . We will calculate only the transformation for the magnetic modes.

The Kelvin transformation T is defined by the expression,

$$(\phi, \theta, \psi) \mapsto (r = \cot(\theta), \Psi, \phi), \quad (\text{A.1})$$

where, in the target, a spherical coordinate system with the latitude Ψ and the longitude ϕ is considered. The image of the ψ -coordinate is calculated explicitly. It is independent of the ϕ -coordinate in the target. The absolute value of the gradient of the function $\cot(\theta)$ determines the module of the conformal transformation T . This scale factor, which is a function in the target, is denoted by K .

The Kelvin transformation transforms a magnetic field \mathbf{B}^{S^3} on the source sphere into the corresponding magnetic field $\mathbb{B} = \frac{T_*(\mathbf{B}^{S^3})}{K^3}$ on the target Euclidean space, where K is the scale factor defined above. This function has an asymptotic $\propto r^2$, where T_* is the translation of the vector by means of the differential of T .

One can see that the mode $\mathbb{B}_B = T_*(\mathbf{B}_B)K^{-3}$ is pointed along the longitude ϕ and looks like a toroidal magnetic mode. The mode $\mathbb{B}_A = T_*(\mathbf{B}_A)K^{-3}$ is pointed in a perpendicular direction along (r, Ψ) -coordinates and looks like a poloidal one. The scale factor K is related to the magnetic volume form $K^3 \mathbf{d}x$ in \mathbb{R}^3 , which has an asymptotic $\propto r^6$ along the radius. Both modes \mathbb{B}_A and \mathbb{B}_B have the asymptotic $\propto r^{-4}$.

The domain at the infinity, where the magnetic volume form is great, is the dielectric with a very large magnetic permeability. The operator curl_K with a domain with various magnetic permeability corresponds to the curl operator on S^3 , which is translated using the Kelvin transformation by the formula,

$$\text{curl}_K : \mathbb{B} \mapsto \text{curl}(K\mathbb{B}), \quad (\text{A.2})$$

where curl is the standard vorticity operator in the flat homogeneous Euclidean space. Therefore, the operator curl_K in the domain with various magnetic permeability keeps the asymptotic of a magnetic mode over the radius and is related with the standard vorticity operator by the formula:

$$\text{curl} : \mathbb{B} \mapsto \text{curl}_K(K^{-1}\mathbb{B}). \quad (\text{A.3})$$

In particular, at the infinity, where $K = K(r) \rightarrow +\infty$, the magnetic modes are almost potential and determine no currents.

Magnetic helicity is kept by T . The helicity is calculated as a improper integral in the form,

$$\chi_{\mathbb{B}} = \int_{\mathbb{R}^3} (\mathbb{A} \cdot \mathbb{B}) K^3 \mathbf{d}x = \chi_{\mathbf{B}} = \int_{S^3} (\mathbf{A} \cdot \mathbf{B}) \mathbf{d}V, \quad (\text{A.4})$$

where $\text{curl}_K(\mathbb{A}) = \mathbb{B}$ and $\text{curl}(K\mathbb{A}) = \text{curl}_K(\mathbb{A}) = K\text{curl}(K^{-3}T_*\mathbf{A}) + \nabla(K) \times K^{-3}T_*(\mathbf{A}) = (\mathbb{B} - \nabla(K) \times \mathbb{A}) + \nabla(K) \times \mathbb{A}$.

A.1 The Arnold inequality

The Arnold inequality [16, Theorem 1.5, Ch. III] for a magnetic field on S^3 is the following:

$$\int_{S^3} (\mathbf{B} \cdot \mathbf{B}) dV \geq \frac{1}{2R} \int_{S^3} (\mathbf{A} \cdot \mathbf{B}) dV = \frac{1}{2R} \chi_{\mathbf{B}}, \quad (\text{A.5})$$

where $\frac{1}{2R}$ is the inverse of the smallest eigenvalue of the curl operator, R is the radius of the sphere, which is a scale factor, and $\chi_{\mathbf{B}}$ is the magnetic helicity.

The Arnold inequality is generalized for a non-bounded conductive domain with the variation of magnetic permeability $K(r)$,

$$\int_{\mathbb{R}^3} (\mathbb{B})^2 K^3 d\mathbf{x} = \int_{S^3} (\mathbf{B})^2 K^{-1} dV \geq \max_{S^3}(K^{-1}) \int_{S^3} (\mathbf{B})^2 dV \geq \frac{1}{2R} \chi_{\mathbf{B}}, \quad (\text{A.6})$$

where r is the distance to the origin and R is scale of a inhomogeneity of the magnetic permeability.

References

- [1] R. D. Peccei and H. R. Quinn, CP Conservation in the Presence of Pseudoparticles, *Phys. Rev. Lett.* **38**, 1440–443 (1977).
- [2] L. D. Duffy, K. van Bibber, Axions as Dark Matter Particles, *New J. Phys.* **11**, 105008 (2009) [arXiv:0904.3346].
- [3] Y. K. Semertzidis and S. Youn, Axion dark matter: how to see it?, *Sci. Adv.* **8**, eabm9928 (2022) [arXiv:2104.14831].
- [4] G. Galanti and M. Roncadelli, Axion-like Particles Implications for High-Energy Astrophysics, *Universe* **8**, 253 (2022) [arXiv:2205.00940].
- [5] D. J. E. Marsh, Axion Cosmology, *Phys. Rept.* **643**, 1–79 (2016) [arXiv:1510.07633].
- [6] J. Barranco and A. Bernal, Self-gravitating system made of axions, *Phys. Rev. D* **83**, 043525 (2011) [arXiv:1001.1769].
- [7] E. W. Kolb and I. I. Tkachev, Axion Miniclusters and Bose Stars, *Phys. Rev. Lett.* **71**, 3051–3054 (1993) [hep-ph/9303313].
- [8] J. Enander, A. Pargner, and T. Schwetz, Axion minicluster power spectrum and mass function, *J. Cosmol. Astropart. Phys.* **12** (2017) 038 [arXiv:1708.04466].
- [9] L. Visinelli and J. Redondo, Axion Miniclusters in Modified Cosmological Histories, *Phys. Rev. D* **101**, 023008 (2020) [arXiv:1808.01879].
- [10] M. Yu. Khlopov, A. S. Sakharov, and D. D. Sokoloff, The nonlinear modulation of the density distribution in standard axionic CDM and its cosmological impact, *Nucl. Phys. B, Proc. Suppl.* **72**, 105–109 (1999) [hep-ph/9812286].

- [11] A. V. Sokolov and A. Ringwald, Electromagnetic Couplings of Axions, arXiv:2205.02605.
- [12] A. Long and T. Vachaspati, Implications of a primordial magnetic field for magnetic monopoles, axions, and Dirac neutrinos, Phys. Rev. D **91**, 103522 (2015) [arXiv:1504.03319].
- [13] M. Dvornikov and V. B. Semikoz, Evolution of axions in the presence of primordial magnetic fields, Phys. Rev. D **102**, 123526 (2020) [arXiv:2011.12712].
- [14] J.-C. Hwang and H. Noh, Axion electrodynamics and magnetohydrodynamics, Phys. Rev. D **106**, 023503 (2022) [arXiv:2203.03124].
- [15] M. Dvornikov, Interaction of inhomogeneous axions with magnetic fields in the early universe, Phys. Lett. B **829**, 137039 (2022) [arXiv:2201.10586].
- [16] V. I. Arnold and B. A. Khesin, *Topological Methods in Hydrodynamics* (Springer, New York, 1998).
- [17] P. Akhmet'ev, S. Candelaresi, and A. Y. Smirnov, Minimum quadratic helicity states, J. Plasma Phys. **84**, 775840601 (2018) [arXiv:1806.07428].
- [18] G. Hornig, and C. Mayer, Towards a third-order topological invariant for magnetic fields, J. Phys. A: Math. Gen. **84**, 3945–3959 (2002) [physics/0203048].
- [19] M. A. Kamchatnov, Topological solitons in magnetohydrodynamics, Sov. Phys. JETP **55**, 69–73 (1982).
- [20] P. Akhmet'ev and I. V. Vyugin, Dispersion of the Arnold's Asymptotic Ergodic Hopf Invariant and a Formula for its Calculation, Arnold Math. J. **6**, 199–211 (2020) [arXiv:1906.12131].
- [21] E. A. Kudryavtseva, Helicity is the Only Invariant of Incompressible Flows whose Derivative is Continuous in the C1 Topology, Math. Notes **99**, 611–615 (2016) [arXiv:1511.03746].
- [22] V. Z. Grines and L. M. Lerman, Nonautonomous dynamics: classification, invariants, and implementation, Contemp. Math. Fund. Directions, **68**, 596–620 (2022), <https://doi.org/10.22363/2413-3639-2022-68-4-596-620>.
- [23] A. Brandenburg, K. Enqvist, and P. Olesen, Large-scale magnetic fields from hydro-magnetic turbulence in the very early universe, Phys. Rev. D **54**, 1291–1300 (1996) [astro-ph/9602031].
- [24] L. Husdal, On Effective Degrees of Freedom in the Early Universe, Galaxies **4**, 78 (2016) [arXiv:1609.04979].
- [25] L. Visinelli, Boson Stars and Oscillatons: A Review, Int. J. Mod. Phys. D **30**, 2130006 (2021) [arXiv:2109.05481].
- [26] P. Charbonneau, Dynamo models of the solar cycle, Living Rev. Solar Phys. **17**, 4 (2020).
- [27] A. V. Gruzinov and P. H. Diamond, Self-Consistent Theory of Mean-Field Electrodynamics, Phys. Rev. Lett. **72**, 1651–1653 (1994).

- [28] Y. Baia and Y. Hamada, Detecting axion stars with radio telescopes, *Phys. Lett. B* **781**, 187–194 (2018) [arXiv:1709.10516].
- [29] M. Buschmann, C. Dessert, J. W. Foster, A. J. Long, and B. R. Safdi, Upper Limit on the QCD Axion Mass from Isolated Neutron Star Cooling, *Phys. Rev. Lett.* **128**, 091102 (2022) [arXiv:2111.09892].
- [30] F. Chadha-Day, J. Ellis, D.J.E. Marsh, Axion Dark Matter: What is it and Why Now?, *Sci. Adv.* **8**, eabj3618 (2022) [arXiv:2105.01406].